ULTRAFINE GRAINED MATERIALS

The achievement of high strength in an Al 6061 alloy by the application of cryogenic and warm rolling

U. G. Kang · H. J. Lee · W. J. Nam

Abstract The ultrafine-grained Al 6061 alloy, which was fabricated by the combination of cryogenic rolling with warm rolling, achieved high ultimate tensile strength of 420 MPa. Compared with the results by other severe plastic deformation methods, the strengthening effect by the combination of cryogenic rolling with warm rolling was found significantly effective. This notable increase of tensile strength was achieved by the formation of finer precipitates during warm rolling. The presence fine precipitates of diameter below 100 nm, in ultrafine-grained matrix, were confirmed with TEM and STEM. The estimated precipitation strengthening by the fine precipitates was approximately 100 MPa. Based on the results, it was found that cryogenic rolling combined with warm rolling would be effective in increasing strength.

Introduction

In recent years, aluminum alloys have attracted considerable attention due to their increased potential as structural materials in the automotive industry or aerospace applications [1–4]. In particular, 6xxx aluminum alloys have attractive properties, such as high strength, formability, weldability, corrosion resistance, and low cost. Therefore, improvements in strength and formability in 6xxx aluminum alloys would accelerate their application to industry as an alternative choice for steels.

To achieve this goal, considerable work has focused on the fabrication of ultra-fine grained (UFG) materials by imposing severe plastic deformation (SPD) processes such as multi-axial compressions/forging (MAC/F) [5], equal channel angular pressing (ECAP) [6–10], cyclic extrusion compression (CEC) [11], accumulative roll-bonding (ARB) process [12–14] and high-pressure torsion (HPT) [15–17]. These processes are effective in achieving both grain refinement and strengthening without the additions of alloying elements.

Meanwhile, cryogenic rolling has been recognized as one of the effective process to produce nano-structured/ultra fine grained materials [18–20]. The suppression of dynamic recovery during deformation at low temperature would preserve a high density of dislocations. The large number of accumulated dislocations can act as potent recrystallization sites during post-deformation annealing. Accordingly, cryogenic deformation would require less plastic deformation to achieve ultrafine grains, compared to the SPD processes. In addition, a combination of cryogenic rolling with warm rolling produced more noticeable improvement in the mechanical properties of a 5052 Al alloy, with a yield strength and ultimate tensile strength of 410 and 452 MP, respectively [21, 22]. The remarkable improvement in the mechanical properties of a 5052 Al alloy was attributed to the formation of fine precipitates during warm rolling after deformation at cryogenic temperature. On the other hand, the improvement in mechanical properties by a combination of cryogenic rolling with warm rolling appears to be more effective in heat treatable 6xxx aluminum alloys than a 5052 Al alloy.

Therefore, this study examined the mechanical behaviors of a 6061 Al alloy subjected to cryogenic rolling followed by warm rolling. In addition, these results were compared with the mechanical properties obtained by other SPD methods.

U. G. Kang · H. J. Lee · W. J. Nam (✉)
School of Advanced Materials Engineering, Kookmin University, 861-1 Jeongneung-Dong, Songbuk-Ku, Seoul 136-702, Korea
e-mail: wjnam@kookmin.ac.kr

Experimental procedures

The commercial 6061 Al alloy used in this study had been following chemical compositions 1.01 mass% Mg, 0.56 mass% Si, 0.22 mass% Fe, 0.24 mass% Cu, 0.02 mass% Mn, 0.01 mass% Zn, 0.06 mass% Cr. Before rolling, the material underwent a solid-solution treatment at 803 K for 2 h followed by water cooling to room temperature by water quenching.

The rolling process was carried out immediately after the solid solution treatment. For the cryogenic rolled and warm rolled samples (CR + WR), a plate, 8 mm in thickness, was rolled to a 45 % reduction at cryogenic temperature and subsequently warm rolled to a 55 % reduction (total reduction of 75 % in thickness). Cryogenic rolling was performed by dipping the plate into liquid nitrogen for at least 15 min before each rolling pass. Warm rolling was carried out at 448 K. Before each warm rolling pass, the sheet was heated at 448 K for 10 min. The cryogenic rolling samples (CR) were rolled with a 75 % reduction at cryogenic temperature. Subsequently, aging was carried out at 448 K for 12 h (CR + Aging).

The Vickers hardness was measured to monitor the hardness variation with aging time (under a 200 g load).

For the tensile tests, the rolled samples were machined into the ASTM subsized specimens with 25 mm gauge length. Uniaxial tensile tests were conducted with an initial strain rate of 3×10^{-3}/s on an INSTRON machine operating at a constant crosshead speed.

The microstructures were examined by transmission electron microscopy (TEM) to examine the precipitation morphology. All TEM specimens were prepared by jet polishing. The thin foils parallel to the transverse cross section of the sheets were prepared by using a conventional jet polishing technique in a mixture of 70 % methanol and 25 % HNO_3 at -30 °C. TEM observations were carried out using a JEOL JEM1210 microscope operated at 120 kV. STEM was conducted using a JEOL JEM-2100F microscope operated at 300 kV.

Results and discussion

Mechanical properties

Figure 1 shows the engineering stress–strain curves of the 6061 Al alloys deformed by different rolling conditions with a thickness reduction of 75 %. The strength of the cryogenic rolled (CR) sample (YS = 313 MPa and UTS = 321 MPa) was much higher than that of the solid solution treated (SST) sample (YS = 102 MPa and UTS = 209 MPa). The accumulated dislocations during plastic deformation at cryogenic temperature and the
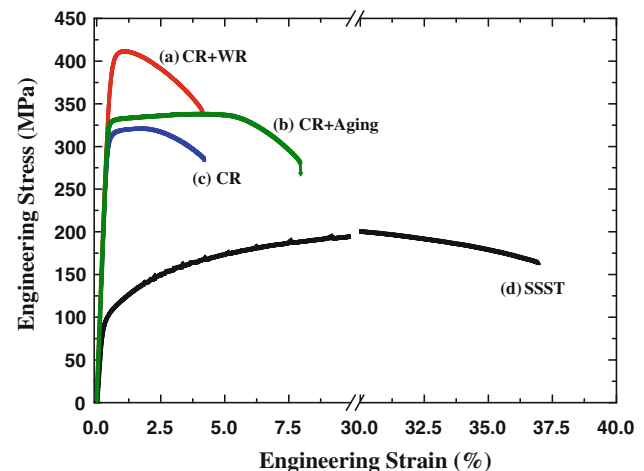

Fig. 1 Stress–strain curves of Al 6061 alloys treated under different conditions; *a* cryogenic temperature rolling and warm temperature (at 448 K) rolling to 75 %, CR + WR, *b* cryogenic temperature rolling to 75 % and aging at 448 K for 12 h, CR + Aging, *c* cryogenic temperature rolling to 75 %, CR, *d* Commercial 6061 Al, supersaturated solid solution treatment (SSST)

effective suppression of cross-slip or climb of dislocations, associated with dynamic recovery, resulted in a high density of dislocations in the CR samples [18–20, 23].

The application of an aging process at 448 K for 12 h, which is the peak aging condition, caused further strengthening in the CR sample. Note that the YS and UTS of a cryogenic rolled and subsequently aged (CR + Aging) sample are 332 and 340 MPa, respectively, which are approximately 225 and 62 % higher than those of the SST sample. Interestingly, the required aging time for the strengthening effect was only 12 h in a CR sample, compared to 24 h for the T6 treatment. The higher density of dislocations and larger fraction of grain boundaries in the CR samples would act as nucleation sites for the formation of β'' intermetallic compounds and result in faster precipitation kinetics [21].

The ultimate tensile strength and yield strength of a cryogenic rolled and subsequently warm rolled (CR + WR) sample are significantly higher than those of the CR + Aging sample. The YS increased from 332 to 408 MPa (22.8 % increase) and the increment of UTS was almost 25 % (from 340 to 420 MPa). This suggests that the application of warm rolling after cryogenic rolling was more effective increasing the strength than the application of aging after cryogenic rolling.

To examine the effect of warm rolling more precisely, Fig. 2 shows the effect of the aging time on hardness of the samples cryo-rolled and subsequently annealed at 448 K. A peak hardness of 126 Hv was observed at 12 h. This maximum hardness was attributed to the formation of precipitates during the aging of a CR sample. Aging beyond 12 h at 448 K resulted in a slight decrease in hardness.
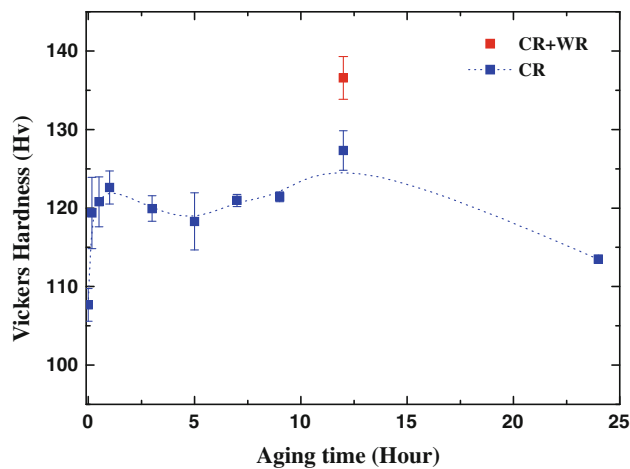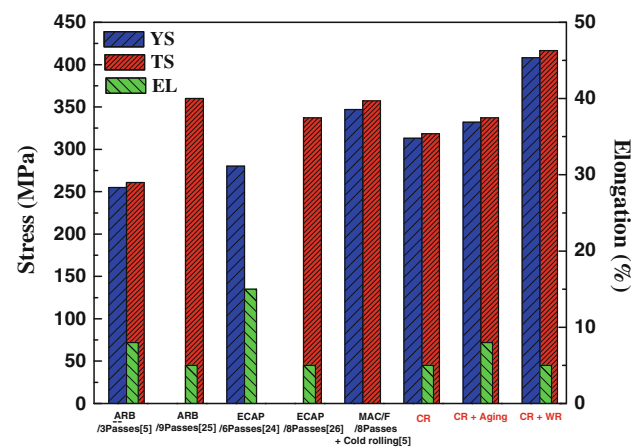
Fig. 2 Vickers micro-hardness versus aging time at 448 K in a Al 6061 alloys, cryorolled with 75 % (CR) and cryorolled and warm rolled (CR + WR)

Fig. 3 Mechanical properties of 6061 Al alloys processed by various SPD methods and current works

A comparison of the peak hardness, 126 and 138 Hv in the CR + Aging sample and CR + WR sample, respectively, shows that the CR + WR process is more effective in improving the strength of Al alloys. The difference between the two samples is the configuration of dislocations generated during plastic deformation and the distribution of precipitates formed during aging or warm rolling. The hardness and UTS in a CR + WR sample was too high to be explained by the contribution of work hardening during warm rolling and the formation of precipitates during inter-pass annealing of warm rolling, compared to 126 Hv and 340 MPa in the CR + Aging sample. This remarkable increase in strength and hardness would most likely be caused by the formation of finer precipitates during warm rolling at 448 K rather than that during static annealing.

The values of total elongation, as well as YS and UTS were compared with the samples processed by severe plastic deformation in Fig. 3. The UTS of a CR + WR sample was notably higher (by ∼57 MPa) than that of the ARB sample with eight passes (UTS = 363 MPa). Nevertheless, they exhibited similar elongation of ∼5 %. This suggests that a combination of cryogenic rolling with warm rolling would become a useful method for achieving superior mechanical properties. This achievement was obtained by only a rolling process without the application of other severe plastic deformation processes.

Microstructures

The above mentioned mechanical properties are closely related to the microstructural evolution. Cryogenic rolling with a 75 % reduction (Fig. 4a) led to the formation of parallel bands of elongated substructures (0.05–0.15 μm in width) with a large density of dislocations. The micro-structure of the CR sample includes dislocation boundaries

inclined at angle ranging from 10 to 30° relative to the rolling plane.

The microstructure of the CR + Aging sample showed a similar trend to that of the CR sample, except for a decrease in the dislocation density due to aging, which is related to static recovery involving the sharpening of low angle boundaries, and the presence of fine particles with a typical size of 30–100 nm (Fig. 4b). Some lamellar sub-structures contained low-aspect-ratio grain fragments. Figure 4c shows the microstructure of a CR + WR sample, consisting of parallel bands of elongated substructures along the rolling direction (100–200 nm in width) with a high density of dislocations. Very small needle-shaped β'' particles, ∼10 nm in diameter, were found near dislocations that would provide preferred nucleation sites for precipitation. This suggests that dynamic aging took place during warm rolling [9].

The microstructure of the sample, cryo-rolled and warm rolled at 448 K (Fig. 5), was examined by STEM and TEM to understand higher strength of a CR + WR sample. Here, the distribution of the precipitates would consist of a mixture of a needle shaped β'' phase with a monoclinic structure (Fig. 5a) and the spherical or rod shaped β' phase (Fig. 5b). In Fig. 5a, fine, needle-shaped, precipitates of β''-Mg_2Si were distributed homogeneously throughout the matrix. The presence of a large number of tiny dots in Fig. 5a represents the β'' needles viewed end-on. The β'' precipitate is closely related to peak-aged conditions and age hardening is caused primarily by the precipitation of the β'' particles. Precipitate refinement in a CR + WR sample is due to the high density of dislocations produced during warm rolling at 448 K, which acts as heterogeneous nucleation sites for the formation of precipitates. The rod-shaped phase β' is typical for an over-aged microstructure. On the other hand, the morphology of the small spherical
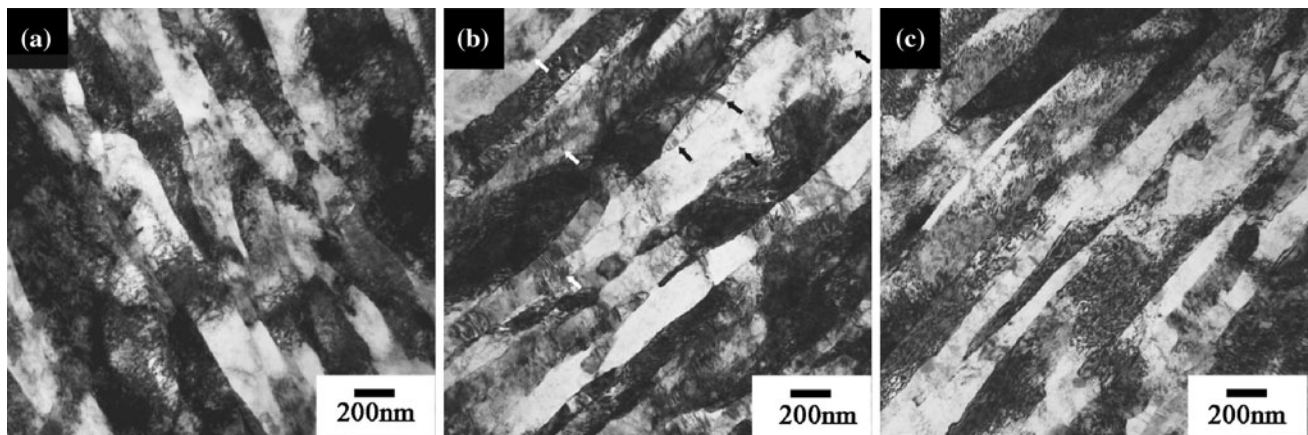
Fig. 4 TEM micrographs the microstructures of Al 6061 alloys; **a** CR, **b** CR + Aging, **c** CR + WR

Fig. 5 Micrographs showing microstructures of 6061 alloy deformed at cryogenic temperature with 45 % reduction and subsequently deformed with 55 % reduction; **a** TEM bright field image (*arrow* indicates precipitates), **b** HAADF STEM mode dark field image
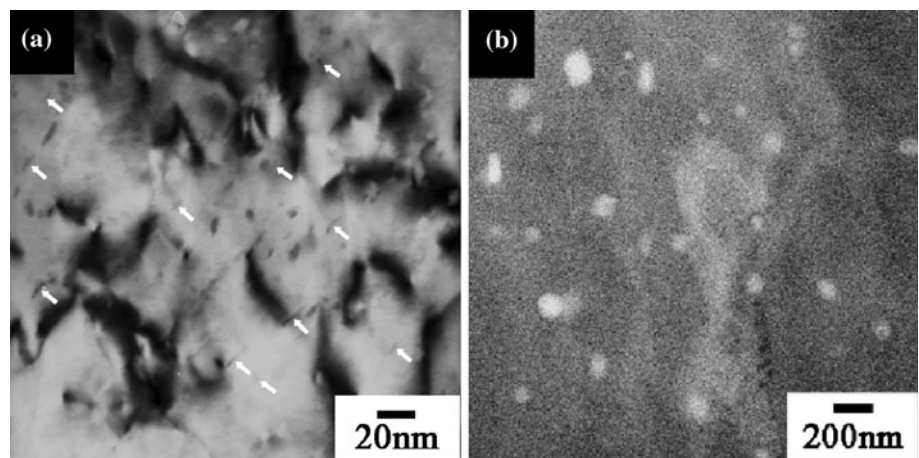
particles in Fig. 5b is not normally observed in conventional 6061 Al alloys. This result agrees with the work reported by Kim et al. [24], who suggested that the preferential nucleation and growth of particles on high-dislocation density regions, where atomic diffusion is expected to be enhanced by pipe diffusion along the cores of dislocations dispersed randomly in the matrix, might allow the precipitates to grow isotropically.

Effect of fine precipitation during warm rolling

The contribution of precipitate strengthening by the formation of β'' and β' fine precipitates during warm rolling can be calculated by subtracting the contribution of solid-solution, dislocation, and grain-refinement from YS (313 MPa) on a CR sample. The obtained contribution of precipitation strengthening was 95 MPa (approximately 100 MPa). An Orowan dislocation looping mechanism is well known as a relationship between the diameter of precipitates and the amount of precipitation-strengthening by Ref. [25] as follows:

$$\Delta\delta_{or} = \frac{M(0.4\,Gb)}{\pi\sqrt{1-v}}\frac{\ln\left(\frac{2r}{b}\right)}{\lambda} \qquad (1)$$

where $M = 3.06$ is the mean matrix orientation factor for aluminum, $v = 0.34$ is the matrix poisson's ratio [26], $G = 25.4$ GPa is the shear modulus of Al at room temperature, and $b = 0.286$ nm is the magnitude of the matrix Burgers vector [27]. λ is the inter-precipitate distance, which was taken as the square lattice spacing in parallel planes and is given by Ref. [28] as follows:

$$\lambda = \left[\left(\frac{3\pi}{4f}\right)^{\frac{1}{2}} - 1.64\right]r \qquad (2)$$

where f is the volume fraction of Mg$_2$Si precipitates and r is the mean precipitate radius.

For the precipitation strengthening of a CR + WR sample, it can be assumed to form needle shaped β'' and spherical or small rod-shaped β' particles. The strength increase of two types (β'' and β') of precipitates was obtained using the relationship between the two diameter and volume fraction of precipitates. The total equilibrium
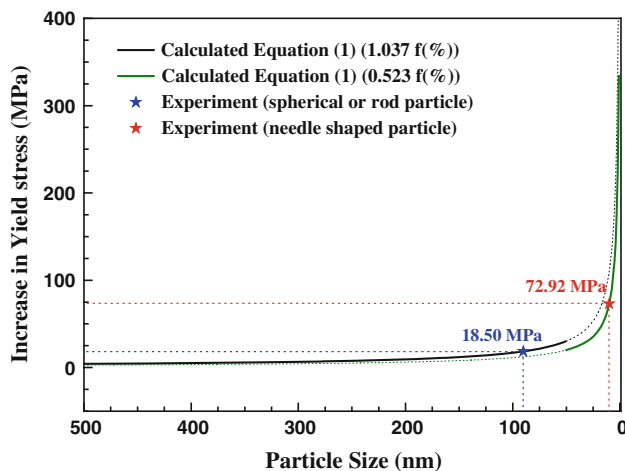
Fig. 6 Increase of yield strength versus precipitate radius and volume fraction in an Al 6061 alloy

phase fraction (1.56 %) was calculated using the computational thermodynamic software Thermo-calc. Subsequently, the volume fraction, f (%), of the spherical or small rod-shaped β' was determined to be 1.037 % from several STEM images of different areas with several hundred precipitates.

Figure 6 shows the relationship between the particle diameter and $\Delta\sigma$. When the mean diameter of the needle shaped β'' was 10 nm with a 0.523 % volume fraction and that of the spherical or small rod β' was 89.92 nm with a 1.037 % volume fraction. The sum of precipitation strengthening was determined to be 91.42 MPa. This is in good agreement with the amount of the subtracted strength for precipitation strengthening (95 MPa).

Therefore, the present study was carried out to examine the mechanical behaviors of a 6061 Al alloy subjected to cryogenic rolling followed by warm rolling.

Conclusions

The mechanical properties of a 6061 Al alloy received cryogenic and warm rolling were investigated. The results are summarized below:

1. A combination of cryogenic rolling and warm rolling was more effective in increasing the strength than cryogenic rolling alone or a cryogenic rolling and aging treatment.
2. The increase in strength in the cryogenic rolled and warm rolled sample was attributed to high density of two types of precipitates. One is a small needle-shaped β'' particle, with ~ 10 nm in size, and the other is a spherical or rod-shaped β' particle (~ 100 nm).
3. The yield strength of a cryogenic rolled and warm rolled sample was higher than a cryogenic rolled sample (~ 100 MPa). This amount of strengthening can be explained by an Orowan dislocation looping mechanism.

References

1. Evancho JW, Kaufman JG (1977) Aluminum 53:609
2. Hatch JE (1984) Properties and physical metallurgy. American Society for Metals, Metals Park
3. Vetrano JS et al (1997) Mater Sci Eng A 238:101–107
4. Troegar LP et al (2000) Mater Sci Eng A 277:102–113
5. Cherukuri B et al (2005) Mater Sci Eng A 410:394–397
6. Valiev RZ et al (1991) Mater Sci Eng A 137:35–40
7. Lee S et al (2002) Acta Mater 50:553–564
8. Chang SY et al (2003) J Alloys Compd 354:216–220
9. Cai M et al (2004) Mater Sci Eng A 373:65–71
10. Zhao YH et al (2004) Acta Mater 52:4589–4599
11. Richert J, Richert M (1986) Aluminum 62:604
12. Tsuji N et al (1999) Scripta Mater 40:795–800
13. Saito Y et al (1999) Acta Mater 47:579–583
14. Park KT et al (2001) Mater Sci Eng A 316:145–152
15. Valiev RZ et al (2006) Prog Mater Sci 51:881–981
16. Harai Y et al (2008) Scripta Mater 58:469–472
17. Edalati K et al (2008) Mater Sci Eng A 497:168–173
18. Wang Y et al (2002) Nature 419:912–915
19. Lee YB et al (2004) Scripta Mater 51:355–359
20. Zhao YH et al (2006) Adv Mater 18:2280–2283
21. Gang UG et al (2009) Mater Trans JIM 50:82–86
22. Kang UG, Lee JC, Jeong SW, Nam WJ (2010) J Mater Sci 45:4739–4744
23. Shanmugasundaram T et al (2006) Scripta Mater 54:2013–2017
24. Kim WJ et al (2007) Mater Sci Eng A 464:23–27
25. Brown LM, Ham PK (1971) In: Kelly A, Nicholson RB (eds) Strengthening methods in crystals. Elsevier, Amsterdam, pp 9–135
26. Meyers MA, Chawla KK (1984) Mechanical metallurgy: principles and applications. Engle Wood Cliffs, Paramus
27. Frost HJ, Ashby MF (1982) Deformation mechanism maps. Pergamon Press, Oxford
28. Nembach E (1997) Particle strengthening of metals and alloys. John Wiley, New York